Tuning Mg^{2+} selectivity: comparative analysis of the photophysical properties of four fluorescent probes with an alkynyl–naphthalene fluorophore

Edward R. H. Walter, J. A. Gareth Williams * and David Parker *

Department of Chemistry, Durham University, South Road, Durham DH1 3LE, UK.

E-mail: ***david.parker@dur.ac.uk***, ***j.a.g.williams@durham.ac.uk***. Supporting information and ORCID(s) from the author(s) for this article are available on the www under ***http://dx.doi.org/10.1002/chem.*** xxxx

Abstract: Four alkynyl-1-naphthyl fluorophores have been synthesised with tri- or pentadentate ligating groups suited to the binding of magnesium. Their photophysical and binding properties for magnesium, calcium and zinc ions have been assessed using absorption, emission and excitation spectroscopy. Each compound has a pK_a value between 6.2 and 5.1 and exhibits no significant pH response around pH 7.2. Enhanced selectivity for Mg^{2+} over Ca^{2+} was observed with a pentadentate phosphinate substituted system, compared to its carboxylate analogue, due to a 10-fold lowering of affinity for the Ca^{2+} ion. In each case, the overall dissociation constants for Mg^{2+} fall in the low mM range.

Introduction

Fluorescence spectroscopy is a powerful and extensively used tool in cell biology, because of its high temporal resolution and sensitivity. Design strategies and principles for the creation of fluorogenic sensors have recently been reviewed, highlighting the need to seek systems that combine a long wavelength of excitation with the desired affinity and selectivity profile. [1] The application of fluorescent sensing is widespread, with a variety of fluorescent sensors providing detailed information on the roles of biologically active cations [2-5] and anions [6] *in vitro* and *in cellulo*. The use of ratiometric probes is highly advantageous, as it allows quantitative information to be obtained independent of environmental factors, such as uneven cell loading or photobleaching. [7] Progress in the development of magnesium-selective fluorescent probes, however, has been slow compared to the monitoring of other divalent

cations, such as Ca^{2+} and Zn^{2+}, resulting in a very limited understanding of the specific details of magnesium homeostasis. [8a] It is worth noting that progress was made in creating sensitive magnesium selective reagents for use in absorption spectroscopy, based on sulfonated hydroxyl-naphthyl chromophores (λ_{abs} 604 nm) that were able to be used with small volumes of bio-fluids. [8b]

Magnesium is the second most abundant divalent cation in cells [9] and is directly involved in a number of intracellular processes, playing a fundamental role in over 600 enzymatic reactions [10] and a key role in the stabilisation of DNA structure.[11] The regulation of 'free' magnesium concentrations in cells is essential, with magnesium imbalance such as the onset of hypomagnesaemia linked to a number of cardiovascular [12], neurodegenerative [13,14] and renal [15] diseases.

The *o*-aminophenol-*N,N,O*-triacetic acid (APTRA) ligand developed by London has been used extensively for a variety of metal ion sensing applications, binding the ionisable 'free' magnesium ion with a K_d value in the low mM range.[16-21] Selectivity is an issue, however, as the APTRA chelates display a much higher affinity towards Ca^{2+} than Mg^{2+} , in every reported case (μM vs mM affinity).[16-21] The ability of APTRA indicators to act as low affinity calcium-based probes has prevented the accurate determination of 'free' Mg^{2+} concentrations in areas where Ca^{2+} concentrations exceed basal levels, such as in serum and in the endo(sarco)plasmic reticulum. The APTRA chelators were first reported over thirty years ago, yet there is still a distinct lack of variety in ligand design for Mg^{2+} sensors. The novelty typically arises from modifications to the chromophore.[18-20] Bidentate β-keto acids, for example, have been examined as alternative probes, and exhibit a higher intrinsic selectivity towards Mg^{2+} over Ca^{2+}. [22-24] The limitation of these β-keto acids arises from the formation of mixed species *in cellulo*, with the probes able to bind to both 'free' Mg^{2+} and $[MgATP]^{2-}$. These adducts are indistinguishable by conventional fluorescence spectroscopic studies. [25]

It is essential that greater effort be placed into the development of new chelate ligand types for the binding of Mg^{2+}, in order to solve this selectivity conundrum. Here, we report the synthesis and analysis of four fluorescent probes containing an alkynyl-naphthalene fluorophore $\mathbf{L^1}$–$\mathbf{L^4}$ (**Figure 1**). Levy *et al* have previously demonstrated that bi-aryl systems containing an APTRA binding group display a ratiometric response to Mg^{2+} and Ca^{2+} ($\mathbf{L^5}$, **Figure 1**). [17] Following addition of Mg^{2+}, for example, a 30 nm hypsochromic shift in the excitation maximum was reported.[17] The development of two new phosphinate-based fluorescent indicators in

particular is described, **L**^{3} and **L**^{4}, as an alternative to the carboxylate-based APTRA binding chelate used in the literature. Using an alkynyl-naphthalene fluorophore, we have attempted to tune magnesium selectivity by changing the position of the oxygen and nitrogen donor groups on the aromatic framework, incorporating a phosphinate at the expense of a carboxylate group, and by modifying the ligand denticity around the metal ion. The incorporation of the four pro-ligands into an alkynyl-naphthalene fluorophore provided an opportunity to analyse the behaviour of the two new phosphinate-based binding groups via fluorescence spectroscopy. It also enabled the fluorescent systems to act as models for lanthanide(III)-based complexes created in parallel work, to be reported elsewhere, in which pyridylalkynylaryl chromophores are also integrated to sensitise lanthanide(III) emission efficiently. [26,27]

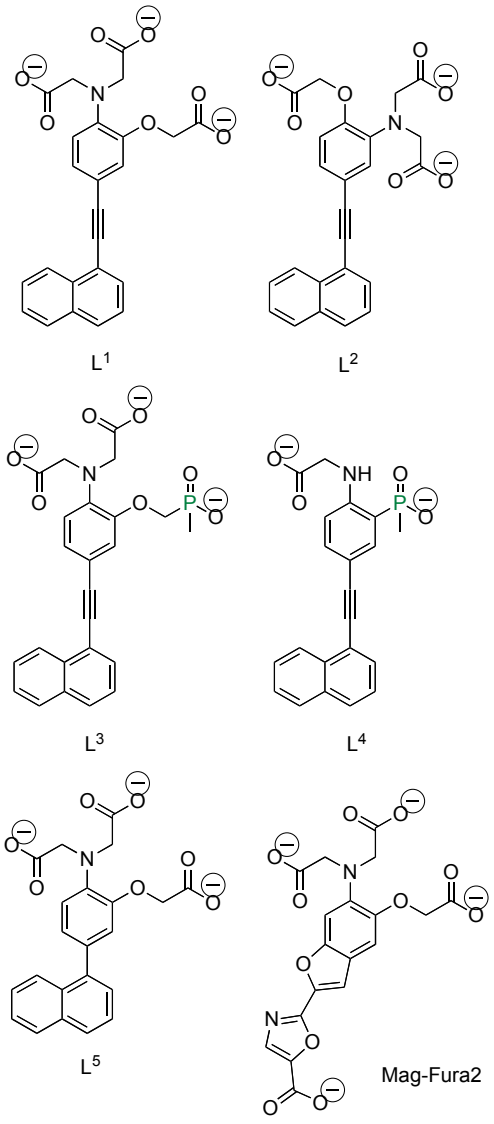

Figure 1. Structures of **L**^{1}–**L**^{4}**,** compared to **L**^{5} , and (*right*) Mag-Fura-2, after London *et al.*[17]

Ligand **L^1** features an APTRA moiety bound to a 1-naphthylalkynyl fluorophore, and **L^2** is constitutionally isomeric with **L^1**, differing in the position of the oxygen and nitrogen donor atoms around the aromatic ring. Ligand **L^3** is a phosphinate analogue of **L^1**, containing a pentadentate APDAP binding chelate. [28] This ligand has very recently been shown to display a dramatically enhanced selectivity for Mg^{2+}, [28] with a 100-fold reduction in the affinity for Ca^{2+} compared to the parent APTRA chelate.[29] Unlike the pentadentate ligands **L^1**–**L^3** that form 5-ring chelates, the tridentate ligand **L^4** forms a [6,5] chelate around divalent metal ions. It has previously been suggested that such a reduction in ligand denticity may inherently favour the binding of the Mg^{2+} cation over Ca^{2+} and Zn^{2+}, as the binding of Ca^{2+} and Zn^{2+} is more enthalpically and entropically driven. [29]

Thus in this work, direct comparisons will be made across the naphthalene series to determine how the change in the position of the donor atoms, the choice of ligating group, denticity and ring chelate size affect affinity and selectivity for Mg^{2+}.

Results and Discussion The synthesis of ligands **L^1**–**L^4** was undertaken using a variety of alkylation and palladium-catalysed cross-coupling reactions. The carboxylate-based ligands, **L^1** and **L^2**, were synthesised from 2-aminophenol and 2-amino-4-bromophenol respectively, as described in the supplementary information (ESI, **Schemes S1** and **S2**). The synthesis of the phosphinate-based ligands **L^3** and **L^4** is described in **Schemes 1** and **2**.

Ligand **L^3** was synthesised from the ethyl ester of the parent structure APDAP, **1**, reported recently in a four-step synthesis from 2-nitrophenol [28] (**Scheme 1**). Selective *para*-bromination of **1** was achieved with [K.18-Crown-6]Br_3 in acetonitrile, [30] yielding **2** in high yield under mild conditions. The (triisopropylsilyl)acetylene (TIPS) group was introduced via a Sonogashira cross-coupling reaction, generating **3** in high yield, from which a one-pot alkyne de-protection with tetrabutylammonium fluoride (TBAF) and palladium-catalysed cross-coupling reaction gave rise to the ethyl ester of **L^3**. Universal ester hydrolysis under basic conditions formed **L^3**, with ligand purity assessed by analytical reverse-phase HPLC.

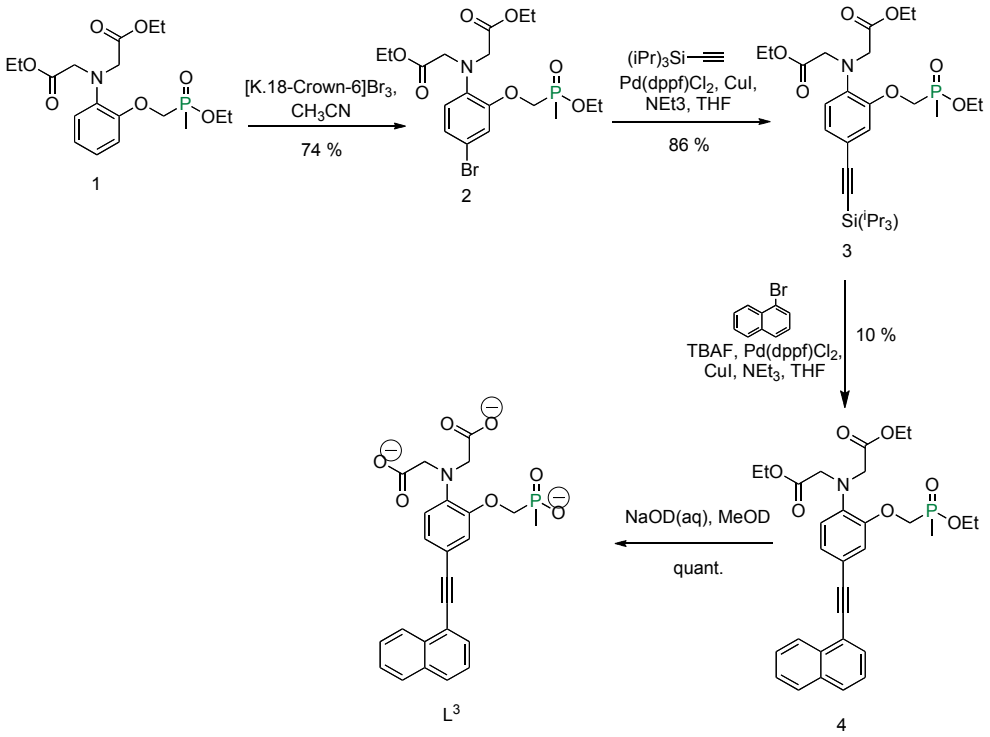

Scheme 1 Synthesis of **L**^{3}

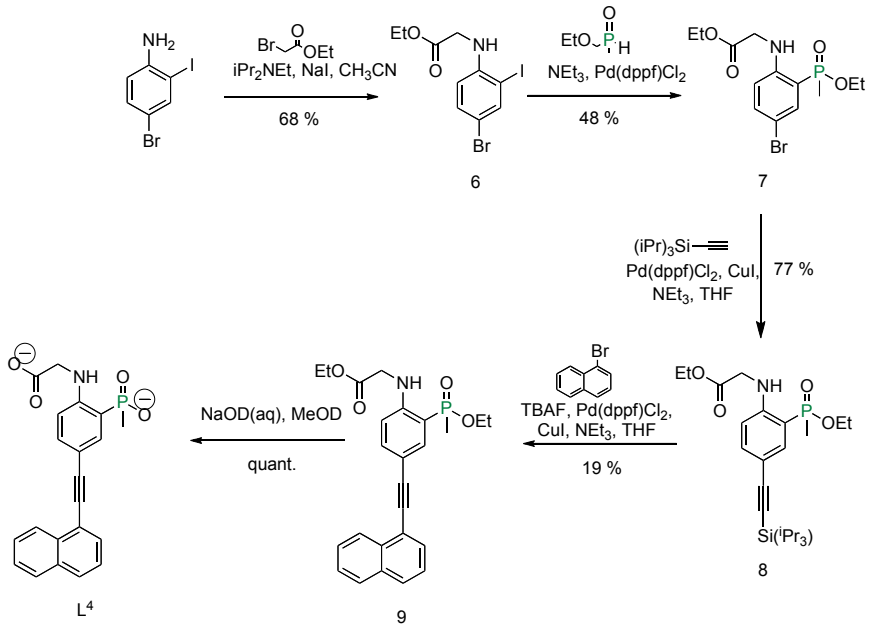

Scheme 2 Synthesis of **L**^{4} from 4-bromo-2-iodoaniline.

The tridentate ligand **L**^{4} was synthesised in five-steps in moderate overall yield (Scheme 2). Alkylation of 4-bromo-2-iodoaniline gave the mono-alkylated intermediate **6** selectively; no traces of *N,N*-di-alkylation were found using a range of conventional base and solvent combinations. The palladium-catalysed coupling of ethyl methylphosphinate with **6** was achieved in a procedure adapted from Parker

and co-workers. [31] Compound **7** formed in moderate yield, and was linked to an alkynyl-naphthalene fluorophore in an identical procedure to **L^3** (**Scheme 1**). Originally, it was hoped that *N,N*-dialkylation would give rise to the formation of a tetradentate chelating ligand, with two carboxylate and one phosphinate oxygen atoms and an aniline nitrogen atom available to bind to metal ions. *N,N*-Di-alkylation was, however, not successful under all conditions attempted, neither from 4-bromo-2-iodoaniline nor from compound **7**, possibly due to steric inhibition of the key substitution reaction caused by the *ortho* iodo or phosphinate substituents.

Photophysical studies of L^1–L^4

The photophysical properties of **L^1–L^4** were examined in aqueous solution at 298K and are summarised in **Table 1**, comparing their behaviour with that of ligand **L^5** developed by London.[17] Ligands **L^1**, **L^3** and **L^4** have large Stokes' shifts, in the range of 166 to 204 nm, nearly 30 nm bigger than with **L^5**, due to the increase in conjugation and the planarity of the alkynyl-naphthalene chromophore. Such large Stokes' shifts are typically found with organic fluorophores that contain an intramolecular charge transfer (ICT) transition and arise from the stabilisation of the excited state by lone pair conjugation involving the *para* aniline nitrogen atom. The excited state of **L^2** in contrast, contains localised π–π* character, due to the weaker electron donating capabilities of the *para* phenolic oxygen atom. A hypsochromic shift in the absorbance, emission and excitation spectra was observed with a much smaller Stokes' shift of 54 nm (**Table 1**). The excitation wavelengths with L^{1,3,4} allow the use of LEDs that operate at 365 nm, and can be pulsed to minimise the energy absorbed by the system under examination.

Table 1. Photophysical data for **L^1–L^5** in H_2O at 298 K. Quantum yields (**Φ**) ± 20 % measured in H_2O.

Ligand	λ_{abs} / nm, ε /10^3 M^{-1}cm^{-1}	Excitation λ_{max} / nm [a]		Emission λ_{max} / nm [a]		Φ_{H_2O} / %
		'free'	Mg^{2+} sat.	'free'	Mg^{2+} sat.	
L^1	354, 14.1(3)	358	320	562[b]	522[b]	0.3[c]
L^2	318, 13.8(6)	318	318	372	372	1.3[d]
L^3	350, 10.7(2)	350	336	550	547	0.7[c]
L^4	341, 12.9(4)	341	341	507	507	0.8[c]
L^5	310,[e] n.d.	325[e]	295[e]	499, 358[e]	499, 358[e]	n.d.

[a] Measurements recorded in 50 mM HEPES, 100 mM KCl, pH 7.21 at 298 K; [b] λ_{ex} = 354 nm. Fluorescence quantum yields were measured using either [c] Quinine sulphate (in 0.5 M H_2SO_4) [32] or [d] POPOP [33] as the standards. [e] Values reported by London [17], ε and Φ were not determined (n.d.).

Spectroscopic studies of ligand pK_a with L^1–L^4

For the overwhelming majority of sensors in the literature incorporating an APTRA binding chelate, the pK_a was not determined, owing to putative instability at low pH on prolonged standing in aqueous solution.[20,29,34] No such problems were encountered in this study, allowing the pH behaviour of **L^1**–**L^4** to be studied via fluorescence spectroscopy. In the case of **L^1**–**L^3** , pK_a values were calculated by fluorescence excitation spectroscopy (**ESI**). A ratiometric response to pH change was observed in acidic solutions of **L^1** (**ESI**, **Figure S1**) and **L^3** (**ESI**, **Figure S2**) following protonation of the aniline N atom, with a non-ratiometric 'turn-on' observed in the excitation spectrum of **L^2** (**ESI**, **Figure S3**). The pK_a of the tridentate ligand **L^4**, was only determined by emission spectroscopy as no pronounced pH sensitivity was seen in its excitation spectrum (**ESI**, **Figure S4**).

Calculated pK_a values for **L^1**–**L^4** all fall in the range of 5.2 to 6.2 (**Table 2**), comparable to those reported for Mag-Fura-2, for which a pK_a value of 5.0 was reported by London *et al*. [21] The fluorescence of each ligand was insensitive to pH from 6.5 to 7.5, indicating that at physiological pH the aniline nitrogen and carboxylate / phosphinate ligating groups are fully de-protonated and available to coordinate to metal ions. [2,21,35]

Table 2. The calculated pK_a values of **L^1**–**L^4** in 100 mM KCl, 298 K, with the error associated to the fitting in parenthesis. The pK_a of Mag-Fura-2 is provided for comparison.

Ligand	pK_a
L^1	6.2(04) [a]
L^2	5.7(05) [a]
L^3	5.2(04) [a]
L^4	5.1(02) [b]
Mag-Fura-2	5.0 [21]

[a,b] pK_a values determined by fluorescence excitation / fluorescence emission spectroscopy respectively.

Fluorescence metal ion binding studies with L^1–L^4

Ligand L^1 In the metal-free state, **L^1** exhibits an excitation maximum at 358 nm. Following addition of Mg^{2+}, Ca^{2+} (**Figure 2**) and Zn^{2+} (**Figure S5**), a ratiometric excitation response was observed, with a pronounced wavelength shift of 38 nm towards the blue (**Table 1**, **Figure 2**). The excitation-based ratiometric behaviour seen here has been reported previously for a number of different cation sensors with Mg^{2+} and Ca^{2+}, [2,17-21] including Mag-Fura-2, where a 35 nm hypsochromic shift was

observed in the metal-bound state. [21] TD-DFT has been used to model the effect of Mg^{2+} binding on the excited state of Mag-Fura-2, revealing that the ICT state is perturbed following Mg^{2+} binding, with elimination of a charge transfer process involving the aniline nitrogen lone pair. The excited state instead possesses localised π–π* character in its metal-bound form, resulting in a drastic change in the spectrum on binding. [35]

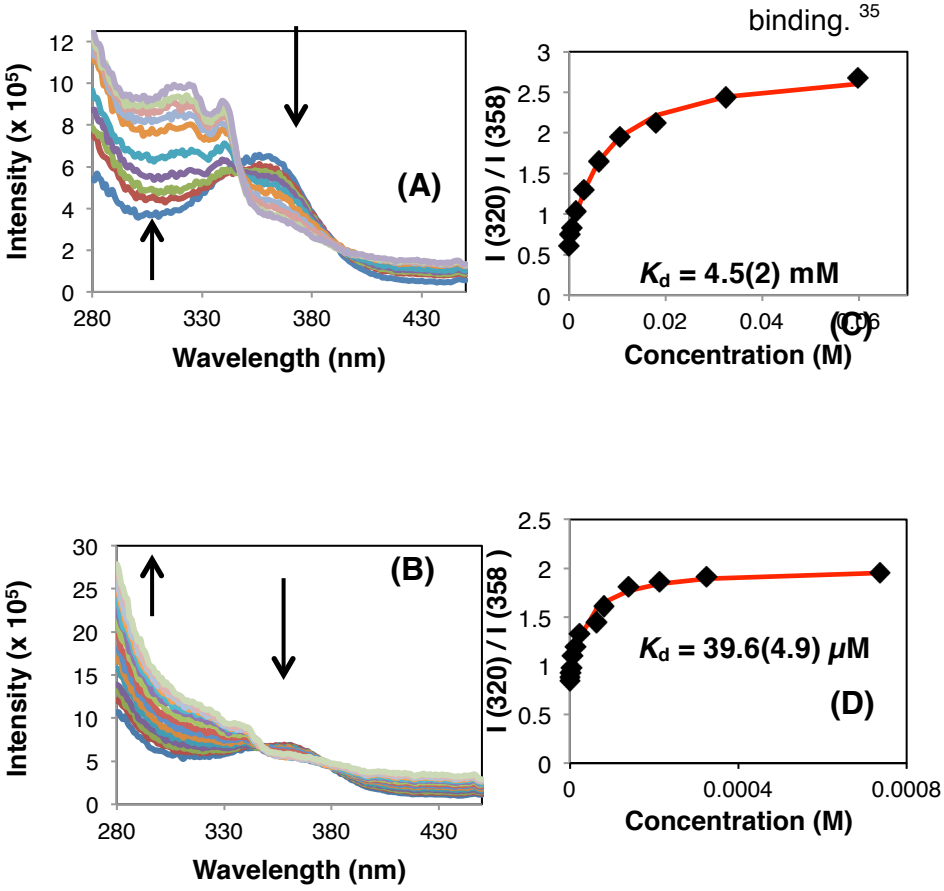

Figure 2. The excitation spectrum of **L[1]** following addition of **(A)** Mg^{2+} and **(B)** Ca^{2+}, λ_{em} = 530 nm, K_d values were calculated from a 1:1 stoichiometry from the ratio of the intensity of the metal-free and bound states against the concentration of **(C)** Mg^{2+} and **(D)** Ca^{2+}, and are reported as an average of two separate metal ion titrations, given with the experimental error in parenthesis. Ligand conc. = 5 μM in 50 mM HEPES, 100 mM KCl, pH 7.21, 298 K.

Dissociation constants of 4.5(2) mM and 39.6(5) μM were calculated following addition of Mg^{2+} and Ca^{2+} respectively (**Table 3**), consistent with typical affinities observed for APTRA analogues in the literature.[17-21] Comparable values were calculated from fluorescence emission spectral changes, with excitation at both the isosbestic point and the wavelength maximum in the absorption spectrum (**ESI**). Following excitation at the isosbestic point (λ_{ex} = 330 nm), 'turn-on' emission ratiometric behaviour was observed (**ESI**, **Figure S6**).

Ligand L² In contrast to the excitation- and emission-based ratiometric behaviour reported for **L¹**, a non-ratiometric 'turn-on' response was found with **L²** following addition of Mg^{2+}, Ca^{2+} and Zn^{2+}. Wavelength maxima of 318 nm and 372 nm were observed in excitation and emission spectra respectively. A 3-, 6- and 9-fold intensity enhancement was found following addition of Mg^{2+}, Ca^{2+} (**Figure 3**) and Zn^{2} (**ESI**, **Figure S7**), owing to the suppression of a photo-induced electron transfer (PET) process. No hypsochromic shift was observed following metal ion binding, as the excited state of **L²** has localised π–π* character in both its 'free' and 'metal-bound' forms.

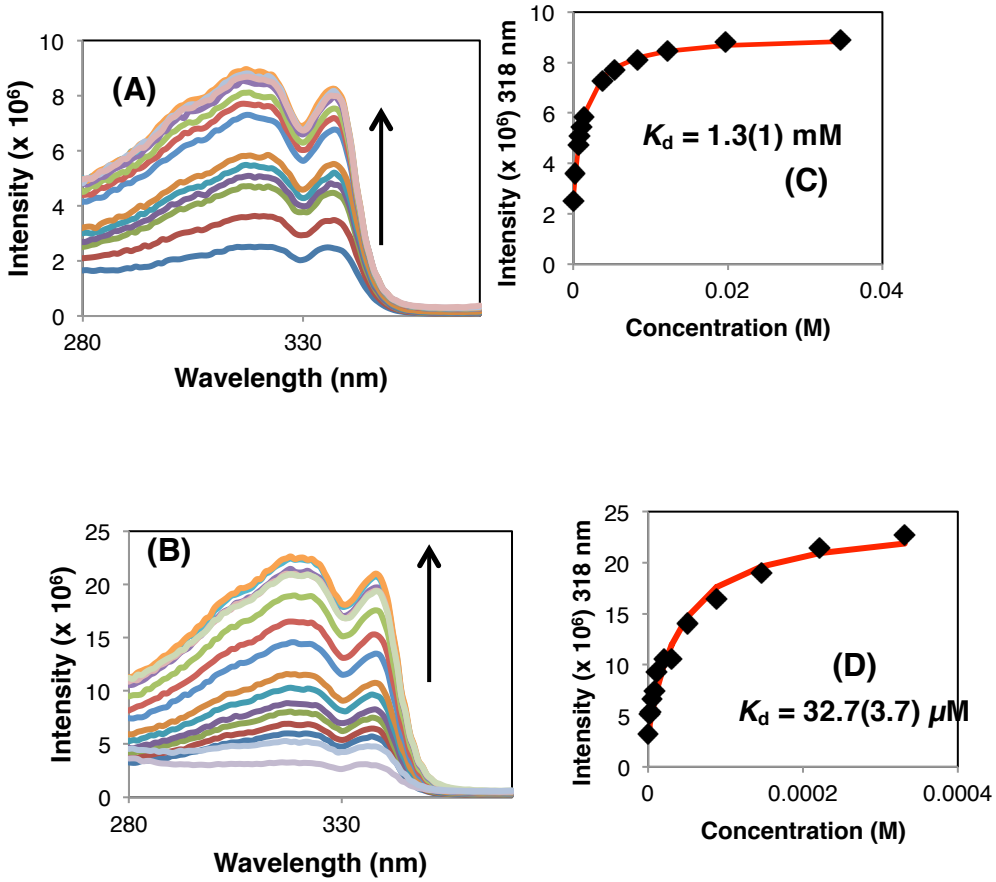

Figure 3. The excitation spectrum of **L²** following addition of **(A)** Mg^{2+} and **(B)** Ca^{2+}, λ_{em} = 377 nm. K_d values were calculated from a 1:1 stoichiometry from the intensity at 318 nm against the concentration of **(C)** Mg^{2+} and **(D)** Ca^{2+}, and are reported as an average of two separate metal ion titrations, given with the experimental error in parenthesis. Ligand conc. = 10 μM in 50 mM HEPES, 100 mM KCl, pH 7.21, 298 K.

Calculated dissociation constants for the binding of **L²** are comparable to those measured for **L¹**. Values of 1.3(8) mM, 32.7(4) μM and 3.2(2) μM were recorded for the binding of Mg^{2+}, Ca^{2+} (**Figure 3**) and Zn^{2+} (**ESI**, **Figure S7**) respectively. The slightly enhanced affinity observed for the binding of **L²** to Mg^{2+} and Ca^{2+} may arise from the increased donor ability of the *meta* aniline nitrogen atom.

It is evident that despite changing the relative position of the nitrogen and oxygen atoms on the APTRA binding framework, comparable affinity and selectivities for Mg^{2+}, Ca^{2+} and Zn^{2+} are found (**Table 3**). However, changing the position of the donor groups does have a significant effect on the excitation and emission spectral response. Both **L[1]** and **L[2]** have dissociation constants in the low mM range following addition of Mg^{2+}, aligning with the concentrations of 'free' Mg^{2+} in mammalian cells (0.8-1.5 mM), [9] and with the affinity and selectivity of alternative APTRA-based sensors reported previously.[17-21] In accordance with literature precedent, ligands **L[1]** and **L[2]** also displayed a higher affinity for Ca^{2+}, responding in the mid-μM range. Such an affinity profile is undesirable for Mg^{2+} sensing applications.[36]

Ligand L[3] The pentadentate APDAP binding chelate was recently developed as an alternative chelating ligand to APTRA. From initial absorbance spectroscopy studies, it was found to display an enhanced selectivity for Mg^{2+}, binding Ca^{2+} in the low mM range.[28] Described here is the first example of incorporation of the APDAP chelate into a fluorescence system to analyse the binding of Mg^{2+}, Ca^{2+} and Zn^{2+}.

Unlike its carboxylate analogue **L[1]**, ligand **L[3]** showed no significant ratiometric behaviour in its absorption or excitation spectra following addition of Mg^{2+} (**ESI**, **Figure S8**). A hypsochromic shift was, however, observed in acidic solution (e.g. at pH 4), suggesting that the aniline nitrogen atom may not have a prominent role in binding to Mg^{2+}. The small changes observed in excitation intensity on addition of Mg^{2+} meant it was not feasible to generate dissociation constants accurately via this method. Instead, K_d values were calculated from fluorescence emission spectral changes. Following excitation at 350 nm, a wavelength maximum of 545 nm was displayed in the 'metal-free' state, with an 18 nm shift to lower wavelengths and a 1.5-fold reduction in the emission intensity on saturation with Mg^{2+} (8.5 mM) (**Figure 4**). Following addition of Ca^{2+} (**Figure 4**) and Zn^{2+} (**ESI**, **Figure S9**), however, an excitation shift was observed that could be followed ratiometrically, with a 31 nm hypsochromic shift in the metal-bound state. Such behaviour implies that the aniline nitrogen atom binds more strongly to Ca^{2+} and Zn^{2+} than to Mg^{2+}.

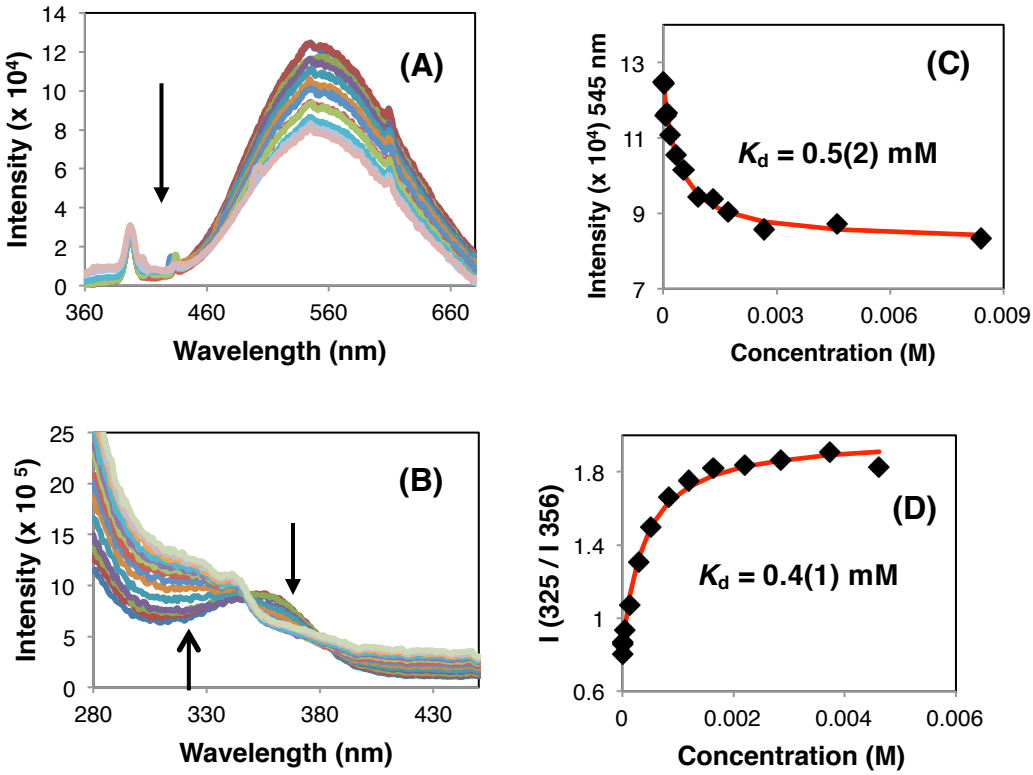

Figure 4. The emission spectrum of $\mathbf{L^3}$ following addition of **(A)** Mg^{2+} (λ_{ex} = 350 nm) and the excitation spectrum following addition of **(B)** Ca^{2+} (λ_{em} = 530 nm). K_d values were calculated from a 1:1 stoichiometry from the intensity plotted against the concentration of **(C)** Mg^{2+} and **(D)** Ca^{2+}, and are reported as an average of three separate metal ion titrations, given with the experimental error in parenthesis. Ligand conc. = 10 μM in 50 mM HEPES, 100 mM KCl, pH 7.21, 298 K.

Dissociation constants of 0.5(2) mM, 0.4(1) mM and 3.3(3) μM were calculated respectively, assuming a 1:1 stoichiometry between Mg^{2+}, Ca^{2+} and Zn^{2+} ions (**Table 3**). The ligand $\mathbf{L^3}$ displays increased selectivity for Mg^{2+} compared to the carboxylate analogues $\mathbf{L^1}$ and $\mathbf{L^2}$. A 10-fold reduction in affinity for Ca^{2+} was found, with a K_d value in the low mM range. It is likely that the increased selectivity is due to the less acute bite angles (9°) around Mg^{2+} in the phosphinate chelate, as predicted from detailed DFT studies of both $[Mg(APTRA)H_2O]^-$ and $[Mg(APDAP)H_2O]^-$. [28] It is both interesting and surprising to note that $\mathbf{L^3}$ has a higher affinity for Mg^{2+} than either $\mathbf{L^1}$ or $\mathbf{L^2}$. Its affinity falls in the desired affinity range, close to the concentration of 'free' Mg^{2+} in mammalian cells.

Ligand L⁴ The tridentate ligand $\mathbf{L^4}$, displayed a non-ratiometric response in both its emission and excitation spectrum, following addition of Mg^{2+}, Ca^{2+} and Zn^{2+}. In the emission spectrum, a wavelength maximum of 499 nm was found, following excitation at 347 nm. Small spectral changes were observed after addition of high

concentrations of Mg^{2+} (160 mM), Ca^{2+} (2 mM) (**Figure 5**) and Zn^{2+} (56 μM) (**ESI**, **Figure S10**). A K_d value of 16.5(6.6) mM was calculated for the binding of Mg^{2+} (**ESI**, **Figure S11**), with the large error associated with fitting small fluorescence intensity changes. Dissociation constants could not reliably be calculated for Ca^{2+} or Zn^{2+}, and weak binding affinity is presumed.

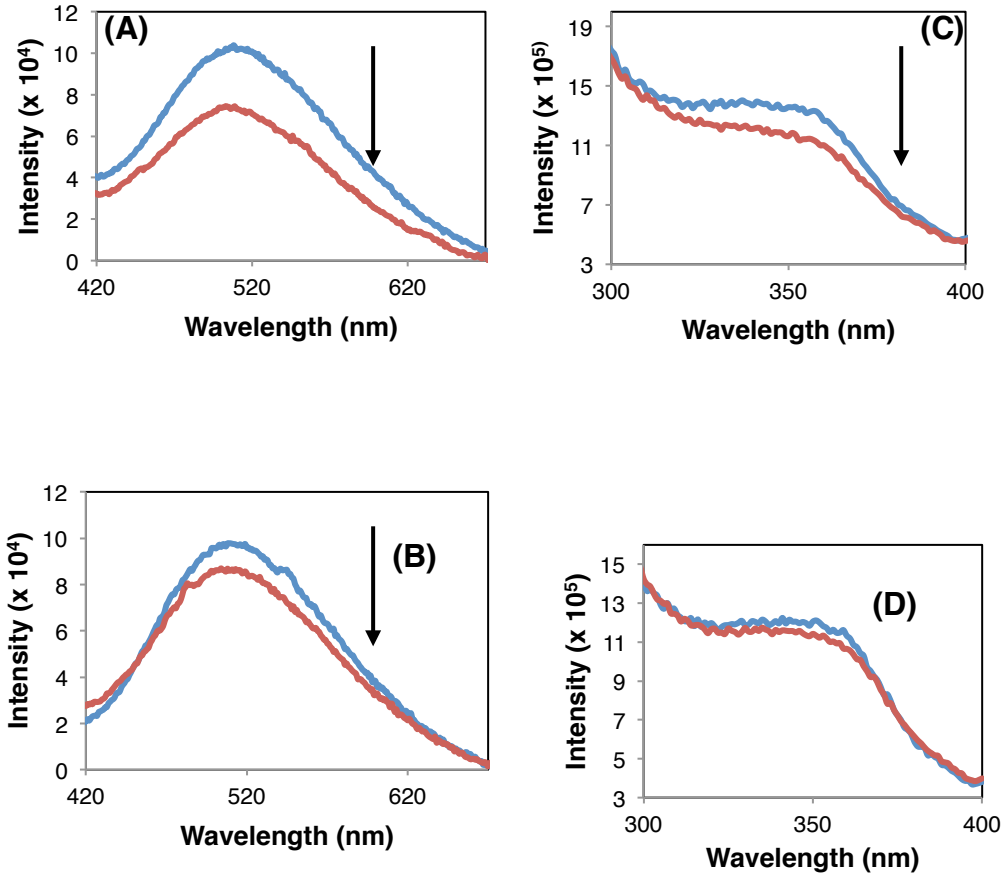

Figure 5. Emission spectra of $\mathbf{L^1}$ following addition of **(A)** Mg^{2+} (160 mM) and **(B)** Ca^{2+} (2 mM) (λ_{ex} = 347 nm). Excitation spectra following addition of **(C)** Mg^{2+} and **(D)** Ca^{2+} (λ_{em} = 501 nm). Ligand concentration = 5 μM in 50 mM HEPES, 100 mM, pH 7.2, KCl, 298K.

It has previously been suggested by Buccella and co-workers that reducing the ligand denticity should favour the binding of Mg^{2+}, as its binding is less enthalpically and entropically driven than Ca^{2+} and Zn^{2+}. [29] In this instance, however, it is apparent that by reducing the number of ligating groups, 4-fold weaker binding is observed for Mg^{2+} compared to that with the pentadentate ligand $\mathbf{L^1}$. The non-ratiometric response and the small intensity changes in the fluorescent emission and excitation spectra following addition of Mg^{2+}, Ca^{2+} and Zn^{2+} make the tridentate $\mathbf{L^4}$ system unsuitable for the accurate determination of the concentrations of metal ions.

Table 3. The calculated dissociation constants for $\mathbf{L^1}$–$\mathbf{L^5}$ (50 mM HEPES,100 mM KCl, pH 7.2, 298 K).

Ligand	K_d (Mg^{2+}) / mM	K_d (Ca^{2+}) / μM	K_d (Zn^{2+}) / μM
$\mathbf{L^1}$	4.5(2)	39.6(4.9)	1.7(1)
$\mathbf{L^2}$	1.3(8)	32.7(3.7)	3.2(2)
$\mathbf{L^3}$	0.5(2)	400(10)	3.3(3)
$\mathbf{L^4}$	16.5(6.6)	‡	‡
$\mathbf{L^5}$	1.8 [17]	17 [17]	n.d.

‡ No dissociation constants were determined from the Ca^{2+} and Zn^{2+} fluorescence titrations due to the absence of significant spectral change. Corresponding K_d values for Mag-Fura-2 are 1.9 mM (Mg^{2+}), 25 μM(Ca^{2+}), 20 nM (Zn^{2+}).

Fluorescence binding studies using $\mathbf{L^3}$ in competitive media

It is thought that 'free' Mg^{2+} concentrations are maintained within the narrow range of 0.7-1.1 mM in the blood plasma, comparable to the concentration of 'free' Mg^{2+} within the majority of mammalian cells.[37] Concentrations of 'free' Mg^{2+} in human serum are often not determined due to the lack of techniques to detect Mg^{2+} ions with sufficient selectivity. [8] The APTRA fluorescent indicators, e.g. Mag-Fura-2, are unsuitable for this task, due to elevated Ca^{2+} levels around 1.1 mM in human serum. [31]

The APDAP-based ligand $\mathbf{L^3}$ possesses many characteristics that render it potentially suitable to detect 'free' Mg^{2+} in human serum. It has no pH interference in the physiological range (pH 6.5-7.5) and exhibits a low mM binding affinity for Ca^{2+} (K_d = 0.4 mM). The binding of Mg^{2+} to $\mathbf{L^3}$ was analysed in a buffered 'competitive medium' containing 50 mM HEPES and concentrations of Na^+ (140 mM), K^+ (4 mM) and Ca^{2+} (1.1 mM) in accordance with the mean values found in human serum. [38] These competitive binding studies were designed to provide an initial indication into how the affinity for Mg^{2+} was affected following competitive cation binding, simulating whether the APDAP chelate would respond to Mg^{2+} fluxes in human serum. A 26 nm hypsochromic shift in the absorbance wavelength maximum was observed, characteristic of partial saturation due to Ca^{2+} binding (**Figure S12**). A wavelength maximum of 545 nm was measured, following excitation at 350 nm, and a 1.6-fold 'turn-off' response was found following addition of 3.5 mM Mg^{2+}, (**Figure 6**).

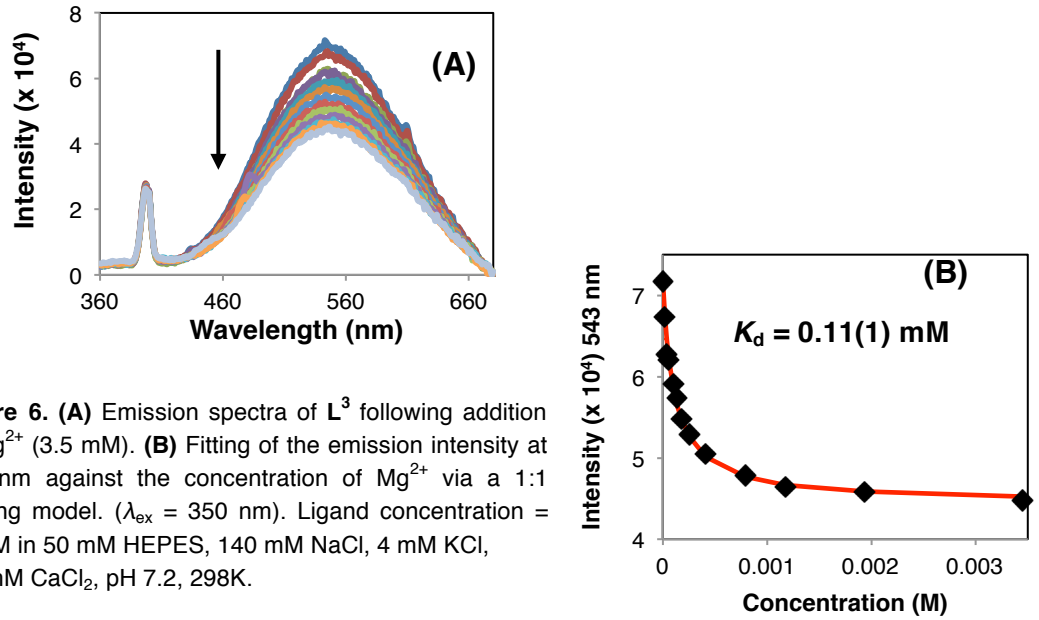

Figure 6. (A) Emission spectra of $\mathbf{L^3}$ following addition of Mg^{2+} (3.5 mM). **(B)** Fitting of the emission intensity at 545 nm against the concentration of Mg^{2+} via a 1:1 binding model. (λ_{ex} = 350 nm). Ligand concentration = 10 μM in 50 mM HEPES, 140 mM NaCl, 4 mM KCl, 1.1 mM $CaCl_2$, pH 7.2, 298K.

A dissociation constant of 0.11(1) mM was calculated for the binding of Mg^{2+} in the buffered medium. Such a significant reduction in apparent affinity was expected due to the presence of 1.1 mM $CaCl_2$ that creates a mixture of unbound and calcium-bound probe in solution, prior to any addition of Mg^{2+}. Nevertheless, this behaviour demonstrates that $\mathbf{L^3}$ can monitor variations in 'free' Mg^{2+} ions in a more complex medium where concentrations of Ca^{2+} are above basal levels. Such an approach is not possible with the APTRA-based sensors, because of the μM binding affinity displayed for Ca^{2+}.

Summary and Conclusions

Following the synthesis of four alkynyl-1-naphthalene fluorophores ($\mathbf{L^1}$–$\mathbf{L^4}$) of differing ligand denticity, we have demonstrated that it is possible to tune Mg^{2+} / Ca^{2+} selectivity. Each ligand possesses a pK_a value in the range 5.1 to 6.2, comparable to that of the commercial probe, Mag-Fura-2. The APTRA analogues, $\mathbf{L^1}$ and $\mathbf{L^2}$, were found to have comparable affinities for both $Mg^{2+}$and Ca^{2+} in the low mM and mid-μM range respectively, supporting literature precedent. Changing the position of the nitrogen and oxygen donor groups, relative to the naphthalene fluorophore, gave rise to significant differences in the absorbance, emission and excitation spectral response to divalent cations. Ligand $\mathbf{L^1}$ displayed a ratiometric response, due to the elimination of the ICT band on protonation and metal ion binding, while a non-ratiometric 'turn-on' response was found for $\mathbf{L^2}$.

By incorporating a phosphinate group into the ligand framework at the expense of a carboxylate group, enhanced Mg^{2+} / Ca^{2+} binding selectivity is created. The APDAP-based ligand, **L^3**, displayed an order of magnitude reduction in affinity for Ca^{2+}, compared to **L^1** and **L^2** with a K_d value of 0.4(1) mM. Such affinity allowed the binding of Mg^{2+} to be investigated in a 'competitive medium', highlighting that **L^3** can be used to monitor variations in 'free' Mg^{2+} concentrations in solutions where Ca^{2+} ions are present above basal levels. In the alkynyl-1-naphthyl systems studied, the pentadentate binding chelates are preferred in order to match the desired low mM affinity for Mg^{2+} binding. Reducing the ligand denticity lowered the affinity for Mg^{2+}; the tridentate ligand **L^4** displayed a 4-fold weaker binding with respect to **L^1**.

This comparative study highlights the advantages of using new ligand types incorporating phosphinate donors in order to significantly change metal ion selectivity. Further work is underway to exploit the differing selectivity profiles of such systems, with different types of signal transduction, seeking systems combining a ratiometric read-out and a longer a wavelength of excitation with the desired magnesium selectivity profile. [1]

Experimental

General procedures

All commercially available reagents were used as received from suppliers, without further purification. All moisture sensitive reactions were carried out under Schlenk-line techniques. The ethyl ester of APDAP, **1**, was synthesised according to our previous work.[28] Thin-layer and column chromatography was performed on silica (Merck Art 5554) and visualised under UV irradiation (254 nm). Routine ^{1}H (400 MHz) and ^{13}C (101 MHz) and ^{31}P (162 MHz) NMR spectra were acquired on Varian Mercury 400 NMR spectrometers. ^{13}C NMR and ^{31}P NMR spectra were run with proton decoupling. Two-dimensional NMR spectra (COSY, HSQC and HSBC) were run on Varian-600 (600 MHz) or VNMRS-700 (700 MHz) instruments. ES-MS data was acquired on a Waters TQD mass spectrometer interfaced with an Acquity UPLC system. Mass spectra of **L^1**–**L^4** were recorded on a Waters Xevo QToF instrument in an acetonitrile and ammonium bicarbonate buffered (25 mM) system.

pK_a Determination

pH measurements were recorded using a Jenway 3510 pH meter in combination with a Jenway 924 005 pH electrode. The pH probe was calibrated before each independent titration using buffer solutions of pH 4, 7 and 10. Samples were prepared with a background of constant ionic strength (I = 0.1 M KCl, 298 K), and titrated to acid. The resulting sigmoidal curve of fluorescence intensity vs. pH was fitted by a non-linear least squares iterative analysis in Boltzmann using Origin 8.0 software. pK_a values were calculated with an error associated with the fitting.

Metal ion binding studies

All divalent metal binding studies for the addition of Mg^{2+}, Ca^{2+} and Zn^{2+} ($[M^{2+}]$) were carried out in buffered solutions of 50 mM HEPES and 100 mM KCl maintained at pH 7.2. All titrations were run in aqueous solution, with water purified by the 'Purite$_{STILL}$plus' system with a conductivity of ≤0.04 μS cm^{-1}. Stock solutions of $[M^{2+}]$ were prepared containing the same concentration of the sensor used in the titration to avoid sample dilution. Absorbance, emission and excitation spectra were run 5 min after the addition of small aliquots of $[M^{2+}]$ to ensure the sample had fully equilibrated. Dissociation constants (K_d values) for the binding of Mg^{2+} and Ca^{2+} were generated from a 1:1 binding model obtained from a least square fitting iterative from *www.supramolecular.org*. In the case of Zn^{2+} binding, K_d's were calculated from a 1:1 binding model from **Equation S3** and **Equation S4** (See **ESI** for more information). Errors associated with the K_d values were generated from two or more repetitions of the binding experiments.

Ligand synthesis

Diethyl 2,2'-((4-bromo-2-((ethoxy(methyl) phosphoryl)methoxy) phenyl) azanediyl)diacetate, (2)

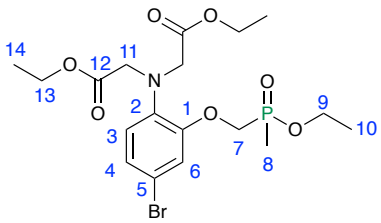

[K.18-crown-6]Br_3 (132.3 mg, 0.24 mmol) was added to a solution of **(1)** (82.5 mg, 0.21 mmol) in anhydrous acetonitrile (1.2 mL). The reaction was stirred at room temperature for 1 h under an inert atmosphere of argon. Reaction completion

was confirmed via ESI mass spectrometry. The solution was diluted with ethyl acetate (10 mL) before being washed with water (10 mL) and dried over $MgSO_4$. The solvent was removed under reduced pressure to form a dark yellow / brown oil. Purification by silica gel column chromatography (gradient 100 % hexane to 100 % ethyl acetate) formed the title compound as a colourless oil. (101 mg, 82 %). ^{1}H NMR (700 MHz, $CDCl_3$) 7.05 (1 H, dd, *J* 9, 2, H^4), 7.00 (1 H, d, *J* 2, H^6), 6.81 (1 H, d, *J* 9, H^3), 4.28 – 4.06 (12 H, m, H^7, H^9, H^{11}, H^{13}), 1.64 (3 H, d, *J* 15, H^8), 1.33 (3 H, t, *J* 7, H^{10}), 1.23 (6 H, t, *J* 7, H^{14}); ^{31}P NMR (283 MHz, $CDCl_3$) + 47.2; ^{13}C NMR (176 MHz, $CDCl_3$) 170.6 (s, C^{12}), 151.4 (d, *J* 12, C^1), 138.6 (s, C^2), 125.5 (s, C^4), 122.0 (s, C^3), 117.7 (s, C^6), 114.7 (s, C^5), 65.1 (d, *J* 110, C^7), 61.0 (d, *J* 7, C^9), 60.8 (s, C^{11} or C^{13}), 53.2 (s, C^{11} or C^{13}), 16.5 (d, *J* 6, C^{10}), 14.1 (s, C^{14}), 12.5 (d, *J* 98, C^8); ESI-LRMS $[C_{18}H_{28}{}^{79}BrNO_7P]^+$ (+) *m/z* 480.1; ESI-HRMS calcd for $[C_{18}H_{28}{}^{79}BrNO_7P]^+$ 480.0787 found 480.0778.

Ethyl 2-({2-[(dimethyl phosphoryl)methoxy]-4-{2-[tris(propan-2-yl)silyl]ethynyl} phenyl}(2-ethoxy-2-oxoethyl)amino)acetate, (3)

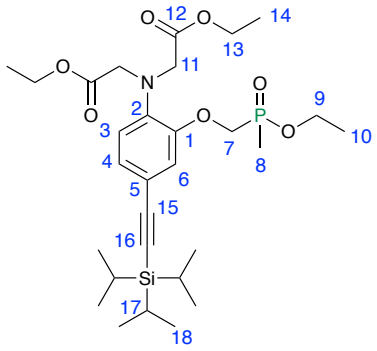

Compound (**2**) (273.9 mg, 0.57 mmol) was dissolved in anhydrous THF (1.8 mL) and the solution was degassed via three freeze-pump-thaw cycles. (Triisopropylsilyl)acetylene (0.64 mL, 2.85 mmol), triethylamine (0.56 mL, 4.02 mmol), $Pd(dppf)Cl_2$ (56.7 mg, 0.08 mmol) and copper iodide (22.0 mg, 0.1 mmol) were added, and the solution was degassed via a further three freeze-pump-thaw cycles. The solution was stirred at 65 ^{o}C for 6 d under an inert atmosphere of argon, reaction completion being determined by ESI mass spectrometry. The solvent was removed under reduced pressure to form a dark brown residue. Purification by silica gel column chromatography (gradient 100 % CH_2Cl_2 to 95 % CH_2Cl_2 / 5 % MeOH) formed the title compound as a pale brown oil (270.9 mg, 86 %). R_f (silica, 95 % CH_2Cl_2 / 5 % MeOH) = 0.54; ^{1}H NMR (600 MHz, $CDCl_3$) 7.08 (1 H, dd, *J* 9, 2, H^4), 6.97 (1 H, d, *J* 2, H^6), 6.81 (1 H, d, *J* 9, H^3), 4.31 –

4.07 (12 H, m, H^7, H^9, H^{11} and H^{13}), 1.65 (3 H, d, *J* 15, H^8), 1.36 (3 H, t, *J* 7, H^{10}), 1.25 (6 H, t, *J* 7, H^{14}), 1.13 (3 H, br m, H^{17}), 1.11 (18 H, s, H^{18}); ^{31}P NMR (243 MHz, $CDCl_3$) + 47.5; ^{13}C NMR (151 MHz, $CDCl_3$) 170.7 (s, C^{12}), 149.9 (s, C^1), 139.8 (s, C^2), 126.8 (s, C^4), 119.9 (s, C^3), 117.5 (s, C^6), 117.4 (s, C^5), 106.6 (s, C^{15}), 89.8 (s, C^{16}), 65.3 (d, *J* 111, C^7), 60.9 (d, *J* 7, C^9), 60.8 (s, C^{11} or C^{13}), 53.3 (s, C^{11} or C^{13}), 18.7 (s, C^{18}), 16.5 (d, *J* 6, C^{10}), 14.2 (s, C^{14}), 12.6 (d, *J* 98, C^8) 11.3 (s, C^{17}); ESI-LRMS $[C_{29}H_{49}NO_7PSi]^+$ (+) *m/z* 582.3; ESI-HRMS calcd for $[C_{29}H_{49}NO_7PSi]^+$ 582.3007 found 582.3016.

Diethyl 2,2'-((2-((ethoxy(methyl)phosphoryl)methoxy)-4-(naphthalen-1-ylethynyl)phenyl)azanediyl)diacetate, (4)

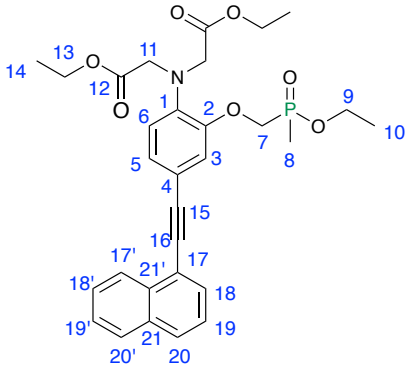

Compound (**3**) (252.5 mg, 0.434 mmol) and 1-bromonaphthalene (58 μL, 0.41 mmol) were dissolved in anhydrous THF (1.8 mL) and the solution was degassed by three freeze-pump-thaw cycles. Triethylamine (1.2 mL), $Pd(dppf)Cl_2$ (43.9 mg, 0.06 mmol) and copper iodide (61.2 mg, 0.32 mmol) were then added and the solution was degassed once more. Tetrabutylammonium fluoride (TBAF, 1 M solution in THF, 0.6 mL, 0.6 mmol) was then added before the brown solution was degassed with three final freeze-pump-thaw cycles. The reaction mixture was stirred at 65 °C for 19 h under an inert atmosphere of argon, before the solvent was removed under reduced pressure to form a dark brown / black residue. Purification by column chromatography (gradient 100 % hexane to 100 % ethyl acetate) formed the title compound as a pale brown oil (24.1 mg, 10 %). ^{1}H NMR (700 MHz, $CDCl_3$) 8.39 (1 H, d, *J* 8, $H^{20'}$), 7.85 (1 H, d, *J* 9, $H^{17'}$), 7.82 (1 H, d, *J* 8, H^{20}), 7.72 (1 H, dd, *J* 7, 2, H^{18}), 7.60 – 7.57 (1 H, m, $H^{19'}$), 7.53 – 7.51 (1 H, m, $H^{18'}$), 7.46 – 7.43 (1 H, m, H^{19}), 7.25 (1 H, dd, *J* 6, 2, H^5), 7.15 (1 H, d, *J* 2, H^3), 6.90 (1 H, d, *J* 8, H^6), 4.36 – 4.09 (14 H, m, H^7, H^9, H^{11} and H^{13}), 1.68 (3 H, d, *J* 15, H^8), 1.37 (3 H, t, *J* 7, H^{10}), 1.26 (6 H, t, *J* 7, H^{14}); ^{31}P NMR (101 MHz, $CDCl_3$) + 53.8; ^{13}C NMR (176 MHz, $CDCl_3$) 170.7 (s, C^{12}), 150.1 (s, C^2), 139.8 (s, C^1), 133.2 (s, C^{17}), 130.2 (s, C^{18}), 128.3 (s, $C^{17'}$), 128.6 (s,

C^{20}), 126.7 (s, $C^{19'}$) 126.5 (s, C^{5}), 126.4 (s, $C^{21'}$), 126.3 (s, $C^{20'}$), 126.2 (s, $C^{18'}$), 125.3 (s, C^{19}), 120.9 (s, C^{21}), 120.0 (s, C^{6}) 117.1 (d, *J* 7, C^{3}) 94.0 (s, C^{15}), 87.0 (s, C^{16}), 64.6 (s, C^{7}, C^{9}, C^{11} or H^{13}), 65.2 (s, C^{7}, C^{9}, C^{11} or H^{13}), 60.9 (s, C^{7}, C^{9}, C^{11} or H^{13}), 53.3 (s, C^{7}, C^{9}, C^{11} or H^{13}), 16.6 (s, C^{10}), 14.2 (s, C^{14}), 12.6 (d, *J* 97, C^{8}); ESI-LRMS $[C_{30}H_{35}NO_7P]^+$ (+) *m/z* 552.1; ESI-HRMS calcd for $[C_{30}H_{35}NO_7P]^+$ 552.2153 found 552.2151.

2,2'-((2-((Hydroxy(methyl)phosphoryl)methoxy)-4-(naphthalen-1-ylethynyl) phenyl)azanediyl)diacetic acid, L^3

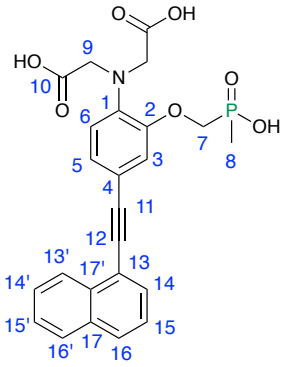

The ethyl ester of **L^3** (**4**) (11 mg, 0.02 mmol) was dissolved in CD_3OD (2 mL) containing NaOD (0.4 M in D_2O, 0.5 mL). The pale yellow solution was stirred under argon at room temperature for 48 h. Ester hydrolysis was confirmed by ^1H NMR spectrometry and ESI-LRMS. The solution was lyophilised to form the title compound as a pale brown solid in quantitative conversion (7 mg). QToF-LRMS $[C_{24}H_{21}NO_7P]^-$ (–) *m/z* 466.1; ESI-HRMS calcd for $[C_{24}H_{21}NO_7P]^-$ (–) 466.1056 found 466.1044. Reverse phase HPLC (0 % - 100 % - 0% CH_3CN in ammonium bicarbonate buffer (25 mM) t_R = 7.1 min; Φ_{H_2O} = 0.7 %.

Ethyl 2-((4-bromo-2-iodophenyl)amino)acetate, (6)

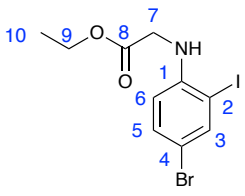

N,N-Diisopropylethylamine (0.96 g, 1.3 mL, 7.50 mmol) and ethyl bromoacetate (600 µL, 5.40 mmol) were added to a solution of 4-bromo-2-iodoaniline (641.4 mg, 2.15 mmol) and sodium iodide (130.2 mg, 2.87 mmol) in anhydrous acetonitrile (3.8 mL). The reaction was heated at 85 °C for 24 h under an inert

atmosphere of nitrogen, before additional *N,N*-diisopropylethylamine (1.2 mL, 6.89 mmol) and ethyl bromoacetate (470µL, 4.24 mmol) were added. The reaction mixture was stirred for a further 40 h at 85 °C. After cooling to room temperature the brown reaction mixture was diluted with ethyl acetate (15 mL), filtered through celite, and washed with water (10 mL) and brine (10 mL). Organic extracts were combined and dried over $MgSO_4$, and the solvent was removed under reduced pressure to form a brown residue. Purification by silica gel column chromatography (gradient 100 % hexane to 80 % hexane / 20 % ethyl acetate) formed the title compound as an off-white solid (565 mg, 68 %). R_f (80 % hexane / 20 % ethyl acetate) = 0.72; m.p. 77 - 78 °C; ^{1}H (700 MHz, $CDCl_3$) 7.77 (1 H, d, *J* 2, H^3), 7.29 (1 H, dd, *J* 9, 2, H^5), 6.29 (1 H, d, *J* 9, H^6), 4.86 (1 H, br t, *J* 5, -NH), 4.26 (2 H, q, *J* 7, H^9), 3.89 (2 H, d, *J* 5, H^7), 1.30 (3 H, t, *J* 7, H^{10}); ^{13}C (176 MHz, $CDCl_3$) 170.0 (C^8), 145.4 (C^1), 140.6 (C^3), 132.1 (C^5), 111.4 (C^4), 109.6 (C^6), 85.3 (C^2), 61.6 (C^7), 46.0 (C^9), 14.1 (C^{10}); ESI-LRMS $[C_{10}H_{11}NI^{79}Br]^+$ (+) *m/z* 384.1; ESI-HRMS calcd for $[C_{10}H_{11}NI^{79}Br]^+$ 383.9096 found, 383.9099.

Ethyl 2-((4-bromo-2-(ethoxy(methyl)phosphoryl)phenyl)amino) acetate, (7)

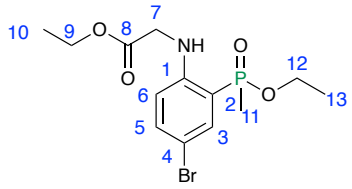

Ethyl 2-((4-bromo-2-iodophenyl)amino)acetate, (**6**) (390.2 mg, 1.02 mmol), ethyl methyl phosphinate (as its EtOH adduct, 200.8 mg, 1.30 mmol) and triethylamine (0.58 mL, 4.16 mmol) were added to dry toluene (degassed by three freeze-pump-thaw cycles). The solution was degassed by a further three cycles before the addition of $Pd(dppf)Cl_2.CH_2Cl_2$ (19.2 mg, 0.024 mmol). The reaction mixture was stirred at 118 °C under an inert atmosphere of argon for 22 h. After cooling to room temperature the solvent was removed under reduced pressure to form a dark brown residue. Purification by silica gel column chromatography (gradient 100 % hexane to 1:1 ethyl acetate / hexane) formed the title compound as a yellow oil (137 mg, 39 %). R_f (silica, 1:1 ethyl acetate / hexane) = 0.52; ^{1}H (600 MHz, $CDCl_3$) 7.50 (1 H, br s, NH), 7.43 (1 H, dd, *J* 12, 2, H^3), 7.38 (1 H, dd, *J* 8, 2, H^5), 6.38 (1 H, dd, *J* 8, 6, H^6), 4.21 (2 H, q, *J* 7, H^9), 4.13 (2 H, m, H^{12}), 3.89 (2 H, br s, H^7), 1.66 (3 H, t, *J* 15, H^{11}), 1.32 (3 H, t, *J* 7, H^{13}), 1.25 (3 H, t, *J* 8, H^{10}); ^{13}C (151 MHz, $CDCl_3$) 170.1 (s, C^8), 150.1 (d, *J* 7, C^1), 136.5 (d, *J* 2, C^5), 134.8 (d, *J* 10, C^3),

114.1 (d, *J* 122, C^2), 113.7 (s, C), 112.9 (d, *J* 10, C^6), 108.0 (d, *J* 15, C^4), 61.3 (s, C^9), 60.9 (d, *J* 7, C^{12}), 45.1 (s, C^7), 16.4 (d, *J* 7, C^{13}), 16.3 (d, *J* 106, C^{11}), 14.2 (s, C^{10}); ^{31}P (243 MHz, $CDCl_3$) + 45.6; ESI-LRMS $[C_{13}H_{19}{}^{79}BrNO_4P]^+$ (+) *m/z* 364.5; ESI-HRMS calcd for $[C_{13}H_{19}{}^{79}BrNO_4P]^+$ 364.0313 found, 364.0320.

Ethyl 2-((2-(ethoxy(methyl)phosphoryl)-4-((triisopropylsilyl)ethynyl)phenyl) amino)acetate, (8)

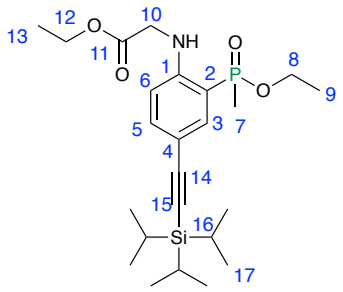

Compound (**7**) (757.0 mg, 2.09 mmol) was dissolved in anhydrous THF (7 mL) and the solution was degassed via three freeze-pump-thaw cycles. (Triisopropylsilyl)acetylene (2.4 mL, 10.7 mmol), triethylamine (2.2 mL, 15.8 mmol), $Pd(dppf)Cl_2$ (157.3 mg, 0.21 mmol) and copper iodide (116.3 mg, 0.61 mmol) were added, and the solution was degassed via a further three freeze-pump-thaw cycles. The solution was stirred at 65 °C for 3 d under an inert atmosphere of argon. Reaction completion was determined by ESI mass spectrometry. The solvent was removed under reduced pressure to form a dark brown residue. Purification by silica gel column chromatography (gradient 100 % hexane to 100 % ethyl acetate 4:1) formed the title compound as a pale brown oil which slowly solidified to a pale brown solid overnight (747 mg, 77 %). m.p = 82 °C – 83 °C; ^1H NMR (600 MHz, $CDCl_3$) 7.71 (1 H, br s, NH), 7.47 (1 H, dd, *J* 14, 2, H^3), 7.42 (1 H, dd, *J* 9, 2, H^5), 6.40 (1 H, dd, *J* 9, 6, H^6), 4.21 (2 H, q, *J* 7, H^{12}), 4.16 – 3.87 (4 H, m, H^8 and H^{10}), 1.68 (3 H, d, *J* 15, H^7), 1.32 (3 H, t, *J* 7, H^9), 1.26 (3 H, t, *J* 7, H^{13}), 1.10 (21 H, s, H^{16} and H^{17}); ^{31}P NMR (243 MHz, $CDCl_3$) + 46.6; ^{13}C NMR (151 MHz, $CDCl_3$) 170.1 (s, C^{11}), 150.8 (d, *J* 7, C^1), 137.6 (d, *J* 2, C^5), 136.5 (d, *J* 10, C^3), 113.4 (d, *J* 123, C^2), 111.3 (d, *J* 14, C^4), 110.7 (d, *J* 10, C^6), 61.3 (s, C^{12}),106.8 (s, C^{14}), 88.5 (s, C^{15}) 60.9 (d, *J*, 6, C^8), 45.0 (s, C^{10}), 18.7 (s, C^{17}), 16.5 (d, *J* 105, C^7), 16.3 (d, *J* 7, C^9), 14.2 (s, C^{13}), 11.3 (s, C^{16}); ESI-LRMS $[C_{24}H_{41}NO_4PSi]^+$ (+) *m/z* 466.2; ESI-HRMS calcd for $[C_{24}H_{41}NO_4PSi]^+$ 466.2543 found 466.2535.

Ethyl 2-((2-(ethoxy(methyl)phosphoryl)-4-(naphthalen-1-ylethynyl)phenyl) amino) acetate, (9)

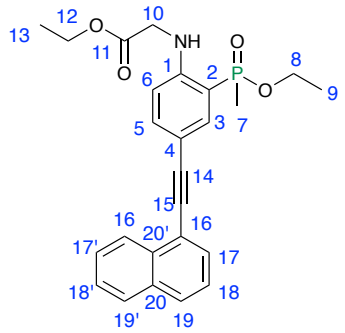

Compound (**8**) (109.7 mg, 0.24 mmol) and 1-bromonaphthalene (31 μL, 0.22 mmol) were dissolved in anhydrous THF (1 mL) and the solution was degassed by three freeze-pump-thaw cycles. Triethylamine (0.7 mL), $Pd(dppf)Cl_2$ (40.6 mg, 0.06 mmol) and copper iodide (42.1 mg, 0.22 mmol) were then added and the solution was degassed once more. Tetrabutylammonium fluoride (TBAF, 1 M solution in THF, 0.35 mL, 0.35 mmol) was then added before the brown solution was degassed with three final freeze-pump-thaw cycles. The reaction mixture was stirred at 65 ^{o}C for 18 h under an inert atmosphere of argon, before the solvent was removed under reduced pressure to form a dark brown / black residue. Purification by column chromatography (gradient 100 % hexane to 100 % ethyl acetate) formed the title compound as a pale orange oil (78 mg, 20 %). ^{1}H NMR (700 MHz, $CDCl_3$) 8.40 (1 H, d, *J* 8, $H^{20'}$), 7.85- 7.83 (2 H, m, $H^{17'}$ and NH), 7.80 (1 H, d, *J* 8, H^{20}), 7.71 (1 H, dd, *J* 7, 1, H^{18}), 7.65 (1 H, dd, J 15, 2, H^{3}), 7.60 – 7.56 (2 H, m, H^{5} and $H^{19'}$), 7.52 – 7.50 (1 H, m, $H^{18'}$), 7.44 – 7.42 (1 H, m, H^{19}), 6.51 (1 H, dd, *J* 9, 6, H^{6}), 4.24 (2 H, q, *J* 7, H^{12}), 4.19 – 3.93 (4 H, m, H^{10} and H^{8}), 1.73 (3 H, d, *J* 15, H^{7}), 1.35 (3 H, t, *J* 7, H^{9}), 1.28 (3 H, t, *J* 7, H^{13}); ^{13}C NMR (176 MHz, $CDCl_3$) 170.1 (s, C^{11}), 151.0 (d, *J* 6, C^{1}), 137.1 (d, *J* 2, C^{5}), 136.2 (d, *J* 10, C^{3}), 133.2 (d, *J* 14, C^{2}), 130.0 (s, C^{18}), 128.3 (s, $C^{17'}$ and C^{20}), 126.6 (s, $C^{19'}$), 126.4 (s, $C^{18'}$), 126.2 (s, $C^{20'}$), 125.3 (s, C^{19}), 121.2 (s, C^{21}), 112.5 (s, $C^{17'}$ or $C^{21'}$), 111.7 (s, $C^{17'}$ or $C^{21'}$), 111.1 (s, C^{4}), 110.0 (d, *J* 10, H^{6}), 94.1 (s, C^{14}), 86.1 (s, C^{15}), 61.4 (s, C^{12}), 60.9 (d, *J* 6, C^{8}), 45.1 (s, C^{10}), 16.44 (d, *J* 106, C^{7}), 16.4 (d, *J* 7, C^{9}), 16.1 (s, C^{13}); ^{31}P NMR (283 MHz, $CDCl_3$) + 46.7; ESI-LRMS $[C_{25}H_{27}NO_7P]^+$ (+) *m/z* 436.4; ESI-HRMS calcd for $[C_{25}H_{27}NO_7P]^+$ 436.1678 found 436.1672.

2-((2-(Hydroxy(methyl)phosphoryl)-4-(naphthalen-1-ylethynyl) phenyl)amino) acetic acid, L^4

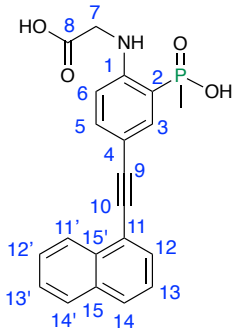

The ethyl ester of **L^4** (**9**) (46.0 mg, 0.10 mmol) was dissolved in CD_3OD (1.8 mL) containing NaOD (0.4 M in D_2O, 0.2 mL). The pale yellow solution was stirred under argon at room temperature for 4 d. Ester hydrolysis was confirmed by ^1H NMR spectrometry, and ESI-LRMS. The solution was then lyophilised to form the title compound as a pale brown solid, in quantitative conversion (30 mg). QToF-LRMS $[C_{21}H_{17}NO_4P]^-$ (-) *m/z* 466.1; ESI-HRMS calcd for $[C_{21}H_{17}NO_4P]^-$ (-) 378.0905 found 378.0895. ^1H NMR (400 MHz, D_2O) 8.19 (1 H, d, *J* 8), 7.69 – 7.60 (3 H, m), 7.48 – 7.47 (1 H, d, *J* 7), 7.43 (1 H, t, *J* 7), 7.36 – 7.21 (4 H, m), 6.27 (1 H, m), 1.32 (3 H, d, *J* 14); ^{31}P (176 MHz, D_2O) + 31.7; Reverse phase HPLC (0 % - 100 % - 0% CH_3CN in ammonium bicarbonate buffer (25 mM)), t_R = 6.6 min; Φ_{H_2O}= 0.8 %.

Acknowledgements We thank EPSRC (EP/ L01212X/1) for generous support.

Key Words Magnesium; fluorescence; selectivity; ligand; calcium

References

[1] (a) X. Li, X. Gao, W. Shi and H. Ma, *Chem. Rev.*, 2014, **114**, 590-659; (b) J. Zhou and H. Ma, *Chem. Sci.*, 2016, **7**, 6309-6315.

[2] G. Grynkiewicz, M. Poenie and R. Y. Tsien, *J. Biol. Chem*. **1985**, 260, 3440-3450.

[3] M. L. Zastrow, R. J. Radford, W. Chyan, C. T. Anderson, D. Y. Zhang, A Loas, T. Tzounopoulos and S. J. Lippard, *ACS Sens*. **2016**, 1, 32-39.

[4] P. J. Dittmer, J. G. Miranda, J. A. Gorski and A. E. Palmer, *J. Biol. Chem*. **2009**, 284, 16289-16297.

[5] K. P. Carter, A. M. Young and A. E. Palmer, *Chem. Rev*. **2014**, 114, 4564-4601.

[6] T. D. Aston, K. A. Joliffe and F. M. Pfeffer, *Chem. Soc. Rev*. **2015**, 44, 4547-4595.

[7] R. M. Paredes, J. C. Etzler, L. T. Watts and J. D. Lechleiter, *Methods*. **2008**, 46, 143-151.

[8] (a) V. Trapani, G. Farruggia, C. Marraccini, S. Iotti, A. Cittadini and F. I. Wolf. *Analyst*, **2010**, 135, 1855-1866; (b) H-M. Ma, Y-X. Huang and S-C. Liang, *Talanta*, 1996, **43**, 21.

[9] A. M. P. Romani, *Arch. Biochem. Biophys.* **2007**, 458, 90-102.

[10] M. Tilmann and F. Wolf, *Curr. Opin. Pediatr*. **2017**, 29, 187-198.

[11] F. I. Wolf, V. Trapani and A. Cittadini, *Magnes. Res*. **2008**, 21, 83-91.

[12] L. M. Resnick, *Am. J. Hypertens*. **1993**, 6, 123S-134S.

[13] J. L. Glick, *Med. Hypothesis*. **1990**, 31, 211-225.

[14] N. Veronese, A. Zurlo, M. Solmi, C. Luchini, C. Trevisan, G. Bano, E. Manzato, G. Sergi and R. Rylander, *Am. J. Alzheimers. Dis. Other. Demen*. **2016**, 31, 208-213.

[15] A. Tin and M. E. Grams. *Kidney. Int.* **2015**, 820-827.

[16] L. A. Levy, E. Murphy, B. Raju and R. E. London, *Biochemistry*. **1988**, 27, 4041-4048.

[17] P. A. Otten, R. E. London and L. A. Levy. *Bioconjugate. Chem*. **2001**, 12, 76-83.

[18] M. S. Afzal, J-P. Pitteloud and D. Buccella, *Chem. Commun*, **2014**, 50, 11358-11361.

[19] G. Zhang, J. J. Gruskos, M. S. Afzal and D. Buccella, *Chem. Sci*. **2015**, 6, 6841-6846.

[20] Q. Lin, J. J. Gruskos and D. Buccella, *Org. Biomol. Chem*. **2016**, 14, 11381-11388.

[21] B. Raju, E. Murphy, L. A. Levy, R. D. Hall and R. E. London, *Am. J. Physiol.* **1989**, 256, 540-548.

[22] P. A. Otten, R. E. London and L. A. Levy. *Bioconjugate. Chem*. **2001**, 12, 203-212.

[23] T. Fujii, Y. Shindo, K. Hotta, D. Citterio, S.Nishiyama, K. Suzuki and K. Oka, *PLOS ONE* **2011**, 6, e23684.

[24] T. Fujii, Y. Shindo, K. Hotta, D. Citterio, S.Nishiyama, K. Suzuki and K. Oka, *J. Am. Chem. Soc*. **2014**, 136, 2374-2381.

[25] S. C. Schwartz, B. Pinto-Pacheco, J-P. Pitteloud and D. Buccella, *Inorg. Chem*. **2014**, 53, 3204-3209.

[26] M. Soulié, F. Latzko, E. Bourrier, V. Placide, S. J. Butler, R. Pal, J. W. Walton, P. L. Baldeck, B. Le Guennic, C. Andraud, J. M. Zwier, L. Lamarque, D. Parker and O. Maury, *Chem. – Eur. J.* **2014**, 20, 8636-8646.

[27] S. Shuvaev, M. Starck and D. Parker, *Chem. – Eur. J.* **2017**, 23, 1-17.

[28] E. R. H. Walter, D. Parker and J. A. G. Williams, *Dalton Trans*. 2018, DOI: 10.1039/c7dt04698g

[29] M. Brady, S. D. Piombo, C. Hu and D. Buccella, *Dalton Trans*. **2016**, 45, 12458-12464.

[30] M. A. Zolfigol, G. Chehardoli, S. Salehzadeh, H. Adams and M. D. Ward, *Tetrahedron Lett*. **2007**, 48, 7969-7973.

[31] J. W. Walton, R. Carr, N. H. Evans, A. M. Funk, A. M. Kenwright, D. Parker, D. S. Yufit, M. Botta, S. De Pinto and K-L. Wong, *Inorg. Chem*. **2012**, 51, 8042-8056.

[32] B. Gelerent, A. Findeissen, A. Stein and J. A. Poole, *J. Chem. Soc. Faraday Trans II*. **1974**, 8, 939-940.

[33] A. M. Brouwer, *Pure. Appl. Chem*. **2001**, 83, 2213-2228.

[34] A. E. Martell, R. J. Motekaitis, A. R. Fried, J. S. Wilson and D. T. MacMillan, *Can. J. Chem,* **1975**, 53, 3771-3776.

[35] G. Zhang, D. Jacquemin and D. Buccella, *J. Phys. Chem. B*. **2017**, 121, 696-705.

[36] A. V. Shmigol, D. A. Eisner and S. Wray, *J. Physiol*. **2001**, 531, 707-713.

[37] J. H. F. Baaij, J. G. J. Hoenderop and R. J. M. Bindels, *Physiol. Rev*. **2015**, 95, 1-46.

[38] D. Parker in 'Crown Compounds Toward Future Applications', ed. S. J. Cooper, VCH, 1992, Chapter 4, pp. 51-69.